Proc. Natl. Acad. Sci. USA
Vol. 91, pp. 13052–13056, December 1994
Physiology

Molecular characterization of an aquaporin cDNA from brain: Candidate osmoreceptor and regulator of water balance

(water channel/vasopressin-secretory neurons/Purkinje cells/ependymal cells/cerebrospinal fluid)

JIN SUP JUNG*, RATAN V. BHAT, GREGORY M. PRESTON, WILLIAM B. GUGGINO, JAY M. BARABAN, AND PETER AGRE†

Departments of Biological Chemistry, Medicine, Neuroscience, and Physiology, Johns Hopkins University School of Medicine, 725 North Wolfe Street, Baltimore, MD 21205

Communicated by Maurice B. Burg, August 29, 1994 (received for review July 14, 1994)

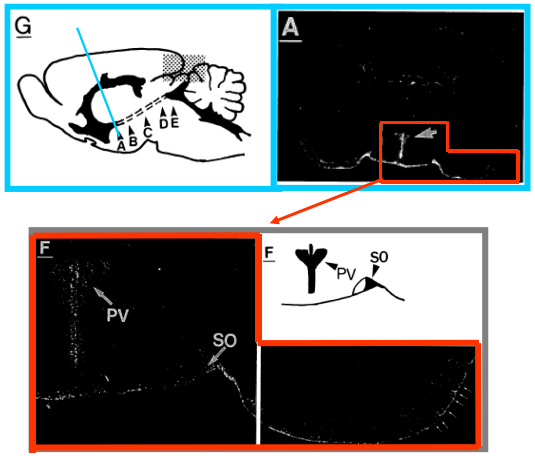

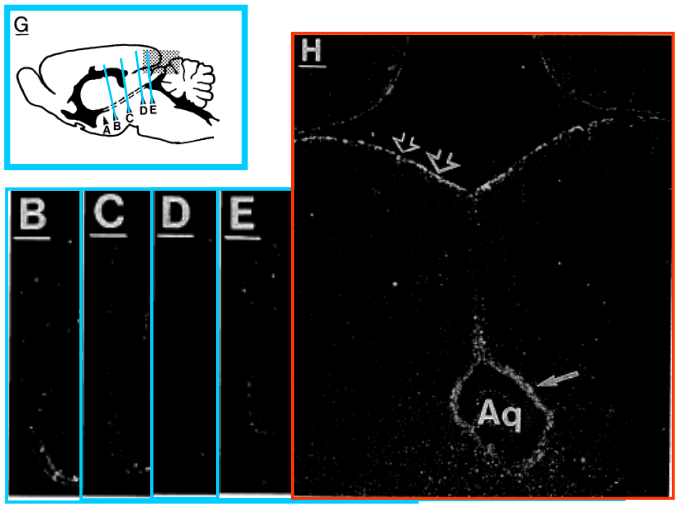

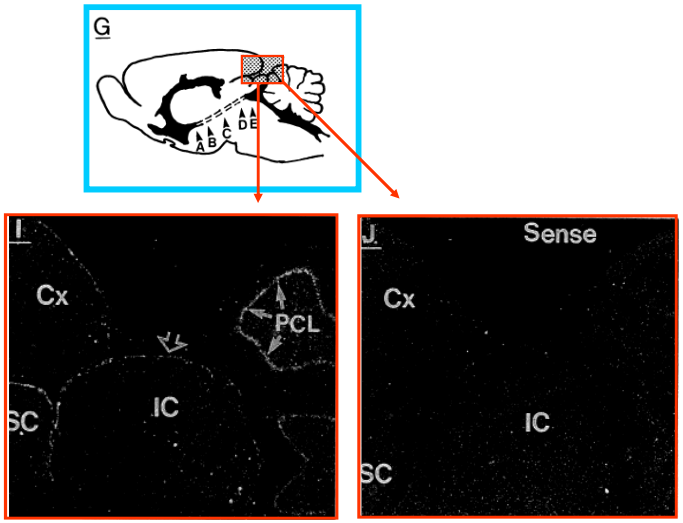

Esistono **due tipi di edema cerebrale**

- **Edema vasogenico**: accumulo di liquido in eccesso nello spazio extracellulare del parenchima cerebrale a causa di aumento di permeabilità della barriera ematoencefalica; segno caratteristico è l'apertura delle giunzioni serrate (*tight junction*) dell'endotelio capillare. Tipico dei tumori cerebrali e delle fasi tardive dell'ictus.

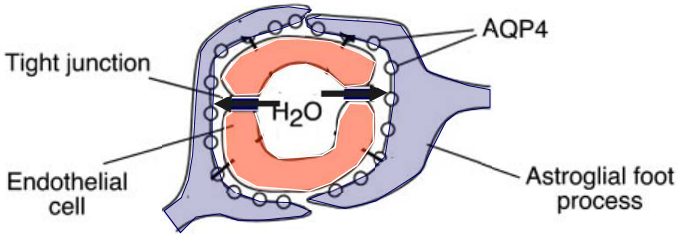

Esistono **due tipi di edema cerebrale**

- **Edema citotossico**: rigonfiamento cellulare che riguarda principalmente le cellule della astroglia, molto evidente nei processi pedicellari (*foot processes*) degli astrociti pericapillari. Tipico delle fasi precoci dell'*ictus* cerebrale su base ischemica e della iponatriemia.

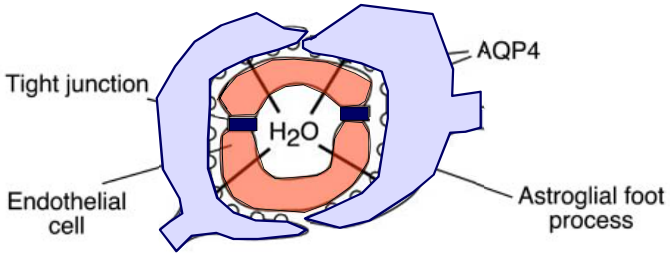

Aquaporin-4 deletion in mice reduces brain edema after acute water intoxication and ischemic stroke

Geoffrey T. Manley[1], Miki Fujimura[2], Tonghui Ma[3], Nobuo Noshita[2], Ferda Filiz[3], Andrew W. Bollen[4], Pak Chan[2] & A.S. Verkman[3]

[1]Department of Neurosurgery, University of California, San Francisco, California 94143, USA
[2]Department of Neurosurgery, Stanford University Medical School, Stanford, California 94305, USA
[3]Departments of Medicine and Physiology, Cardiovascular Research Institute, University of California, San Francisco, California 94143, USA, and [4]Department of Pathology, University of California, San Francisco, California 94143, USA
Correspondence should be addressed to G.T.M.; email: manley@itsa.ucsf.edu; http://www.ucsf.edu/verklab

Nature Medicine (2000) 6, 159-163

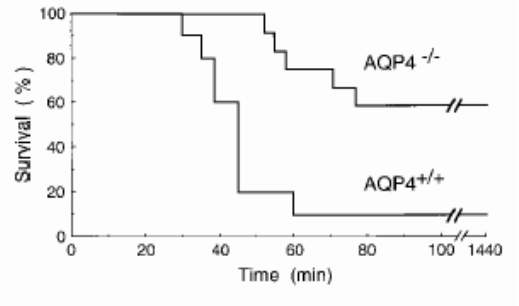

Fig. 1 Effect of water intoxication on survival in AQP4$^{+/+}$ and AQP4$^{-/-}$ mice. Mice received intraperitoneal injection of distilled water (20% body weight) containing DDAVP. Neurological deficit scores were determined at intervals over the first 90 min (see text) and time of death was recorded. Mice were followed for 24 h (1440 min). The percentage of surviving AQP4$^{+/+}$ and AQP4$^{-/-}$ mice is shown for each time point.

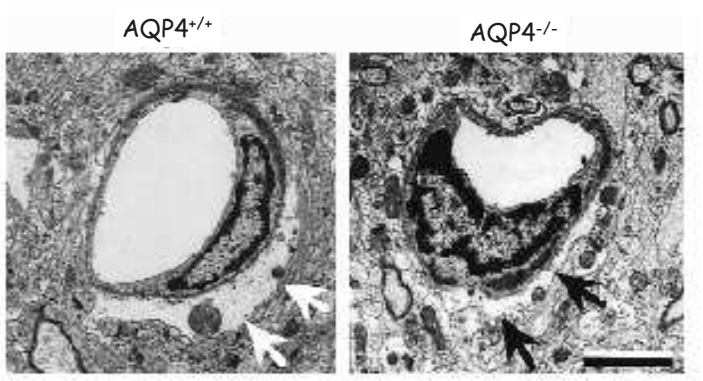

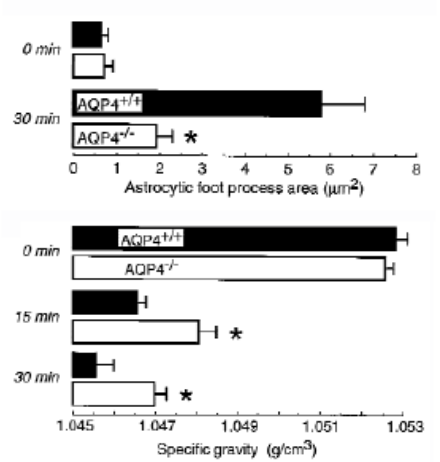

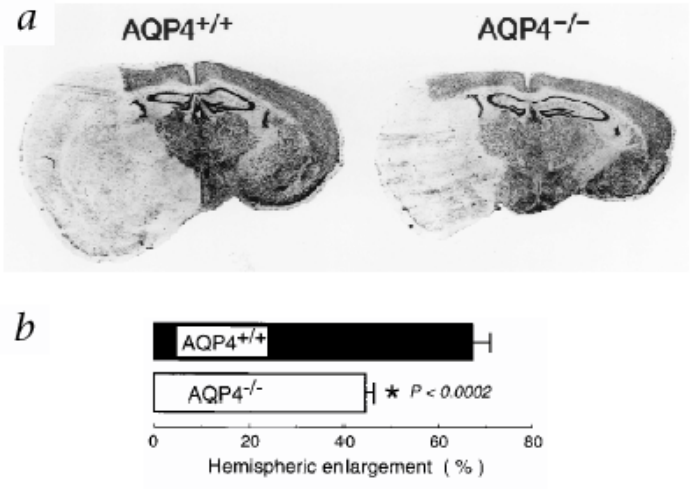

THE JOURNAL OF BIOLOGICAL CHEMISTRY
© 2005 by The American Society for Biochemistry and Molecular Biology, Inc.

Vol. 280, No. 14, Issue of April 8, pp. 13906–13912, 2005
Printed in U.S.A.

Aquaporin-4 Gene Disruption in Mice Reduces Brain Swelling and Mortality in Pneumococcal Meningitis*

Received for publication, December 3, 2004, and in revised form, January 31, 2005
Published, JBC Papers in Press, February 4, 2005, DOI 10.1074/jbc.M413627200

Marios C. Papadopoulos and A. S. Verkman‡

From the Departments of Medicine and Physiology, Cardiovascular Research Institute, University of California, San Francisco, California 94143-0521

The astroglial water channel aquaporin-4 (AQP4) facilitates water movement into and out of brain parenchyma. To investigate the role of AQP4 in meningitis-induced brain edema, *Streptococcus pneumoniae* was injected into cerebrospinal fluid (CSF) in wild type and AQP4 null mice. AQP4-deficient mice had remarkably lower intracranial pressure (9 ± 1 *versus* 25 ± 5 cm H_2O) and brain water accumulation (2 ± 1 *versus* 9 ± 1 μl) at 30 h, and improved survival (80 *versus* 0% survival) at 60 h, through comparable CSF bacterial and white cell counts. Meningitis produced marked astrocyte foot process swelling in wild type but not AQP4 null mice, and slowed diffusion of an inert macromolecule in brain extracellular space. AQP4 protein was strongly up-regulated in meningitis, resulting in a ~5-fold higher water permeability (P_f) across the blood-brain barrier compared with non-infected wild type mice. Mathematical modeling using measured P_f and CSF dynamics accurately simulated the elevated lower intracranial pressure and brain water produced by meningitis and predicted a beneficial effect of prevention of AQP4 up-regulation. Our findings provide a novel molecular mechanism for the pathogenesis of brain edema in acute bacterial meningitis, and suggest that inhibition of AQP4 function or up-regulation may dramatically improve clinical outcome.

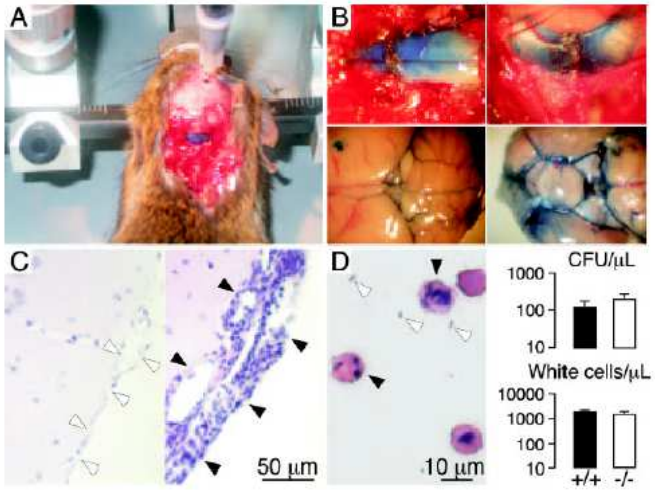

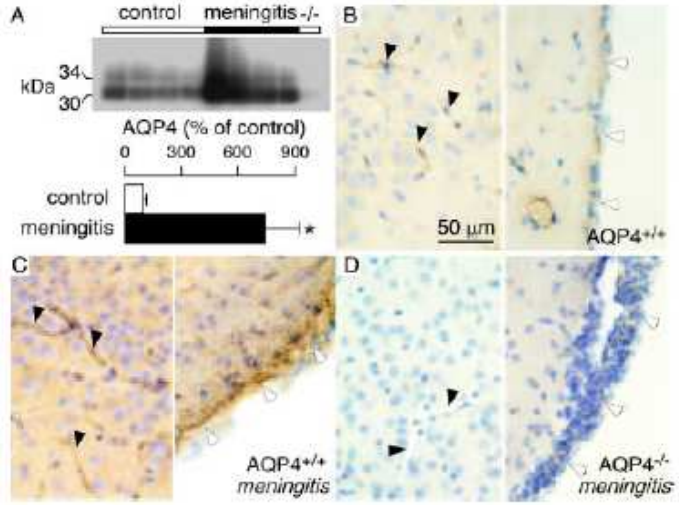

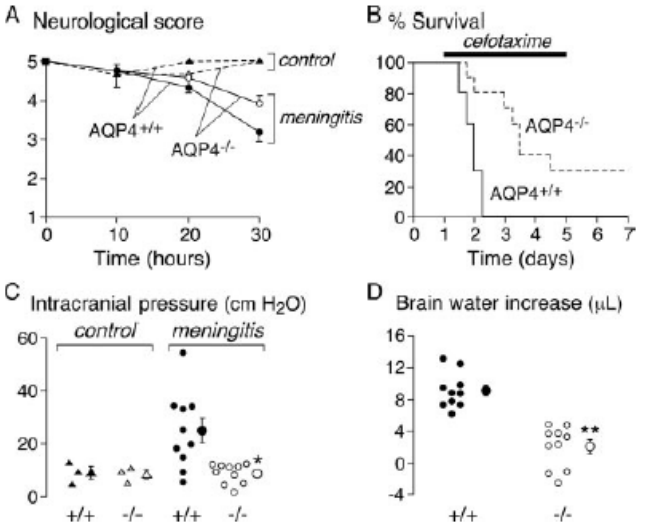

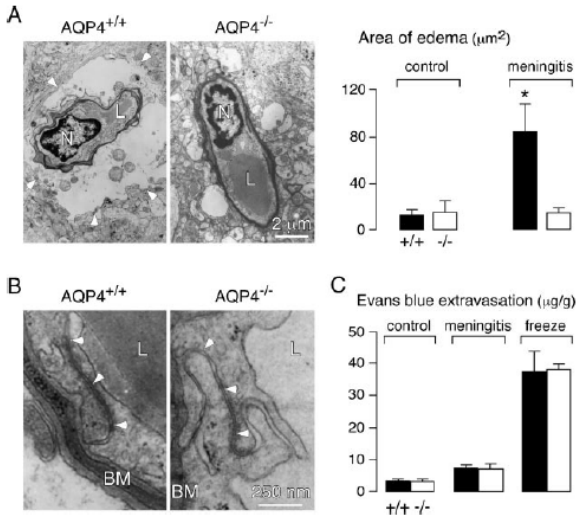

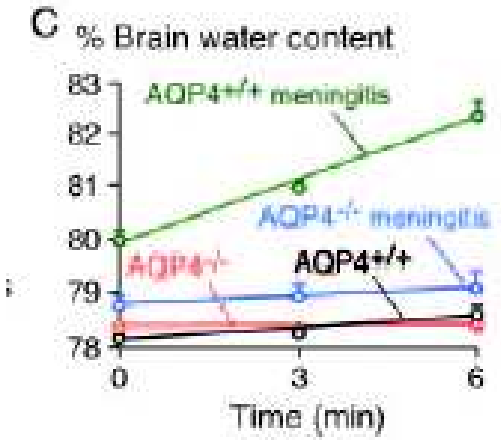

Esistono **due tipi di edema cerebrale**

- **Edema citotossico**: rigonfiamento cellulare che riguarda principalmente le cellule della astroglia, molto evidente nei processi pedicellari (*foot processes*) degli astrociti pericapillari. Tipico delle fasi precoci dell'*ictus* cerebrale su base ischemica, della iponatriemia **e della meningite batterica sperimentale.**

- **Edema vasogenico**: accumulo di liquido in eccesso nello spazio extracellulare del parenchima cerebrale a causa di aumento di permeabilità della barriera ematoencefalica; segno caratteristico è l'apertura delle giunzioni serrate (*tight junction*) dell'endotelio capillare. Tipico dei tumori cerebrali e delle fasi tardive dell'ictus.

PNAS | **May 5, 2009** | vol. 106 | no. 18 | **7437–7442**

Crystal structure of human aquaporin 4 at 1.8 Å and its mechanism of conductance

Joseph D. Ho[a,b], Ronald Yeh[b], Andrew Sandstrom[b], Ilya Chorny[b], William E. C. Harries[b], Rebecca A. Robbins[b], Larry J. W. Miercke[b], and Robert M. Stroud[a,b,1]

[a]Graduate Program in Chemistry and Chemical Biology and [b]Department of Biochemistry and Biophysics, Genentech Hall, University of California, 600 16th Street, San Francisco, CA 94158-2517

Aquaporin (AQP) 4 is the predominant water channel in the mammalian brain, abundantly expressed in the blood–brain and brain–cerebrospinal fluid interfaces of glial cells. Its function in cerebral water balance has implications in neuropathological disorders, including brain edema, stroke, and head injuries. The 1.8-Å crystal structure reveals the molecular basis for the water selectivity of the channel. Unlike the case in the structures of water-selective AQPs AqpZ and AQP1, the asparagines of the 2 Asn-Pro-Ala motifs do not hydrogen bond to the same water molecule; instead, they bond to 2 different water molecules in the center of the channel. Molecular dynamics simulations were performed to ask how this observation bears on the proposed mechanisms for how AQPs remain totally insulating to any proton conductance while maintaining a single file of hydrogen bonded water molecules throughout the channel.

On a structural level, AQP4 is unique among AQPs that it exists in 2 isoforms owing to the use of 2 different translation initiation sites at methionine M1, or at M23. The M1 and M23 isoforms have very different effects on array formation with the shorter isoform favoring larger arrays mediated by 2 symmetric interactions between Arg-108 of each molecule and Tyr-250 of another molecule in the neighboring tetramer (12, 13). The C-terminal 3 amino acids, −SSV, serve as the ligand of a PDZ binding partner, α-syntrophin, which is a component of the dystrophin protein complex that links AQP4 to the actin cytoskeleton (14). Such bridged connection between AQP4 and the actin cytoskeleton allows AQP4 to be anchored at the endfeet of astrocytes such that transgenic mice deficient in α-syntrophin completely lack such polarized expression in astrocytes (15).

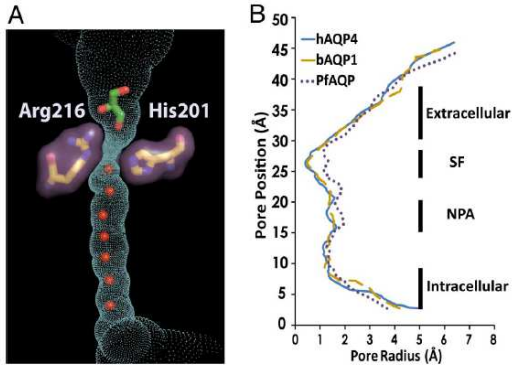

Fig. 2. The conducting pore. The trace of the pore inner surface is shown in cyan. The selectivity filter residues, Arg-216 and His-201, are shown as sticks with surfaces in purple. The glycerol molecule is shown as green stick, and the water molecules in the channel are shown as red spheres. (*B*) Plot of the channel radius versus position along the pore for human AQP4, bovine AQP1 (bAQP1), and the *P. falciparum* AQP (PfAQP). Regions of the channel are labeled as extracellular vestibule, the selectivity filter (SF), the NPA motif, and the intracellular vestibule. The pore inner surface and its dimension are calculated using Hole 2.0 (51).

Extracellular Vestibule, Selectivity Filter, and Conducting Pore. AQP4 is a water-selective channel. Signature to the water-selective channels, His-201 lies directly in the selectivity filter, reducing the channel diameter to ≈1.5 Å, sterically excluding the passage of glycerol (Fig. 2). AQP4 was purified and crystallized in the presence of 5% (vol/vol) glycerol (0.7 M), and 3 glycerol molecules are found in the extracellular vestibule, although not in the selectivity filter where the 2 glycerol-conducting AQPs, GlpF, and PfAQP, bind glycerol identically to one another (26, 27) (Fig. S5). In the water-selective rAQP1, the double mutant Phe56Ala and His180Ala (Phe-77 and His-201 in hAQP4) (Fig. S5) allows for the passage of glycerol, showing that steric occlusion is one mechanism for exclusion of larger solutes (28).

The ≈25-Å long conducting pore contains a line of water molecules and no solute molecule. However, the electron density of

AQP4 is not sensitive to inhibition by mercury (16), because it does not have the reactive cysteine residue in the lumen of the channel corresponding to Cys-191 in AQP1 (17). AQP4 conductance is reduced >50% by phosphorylation mediated by protein kinase C at Ser-180 (18, 19), and increased ≈40% by protein kinase G activity at Ser-111 (20). The gating mechanism by phosphorylation events may be similar to that of the spinach AQP SoPIP2;1 (21, 22).

Swelling of the brain or spinal cord (CNS edema) affects millions of people every year. All potential pharmacological interventions have failed in clinical trials, meaning that symptom management is the only treatment option. The water channel protein aquaporin-4 (AQP4) is expressed in astrocytes and mediates water flux across the blood-brain and blood-spinal cord barriers. Here we show that AQP4 cell-surface abundance increases in response to hypoxia-induced cell swelling in a calmodulin-dependent manner. Calmodulin directly binds the AQP4 carboxyl terminus, causing a specific conformational change and driving AQP4 cell-surface localization. Inhibition of calmodulin in a rat spinal cord injury model with the licensed drug trifluoperazine inhibited AQP4 localization to the blood-spinal cord barrier, ablated CNS edema, and led to accelerated functional recovery compared with untreated animals. We propose that targeting the mechanism of calmodulin-mediated cell-surface localization of AQP4 is a viable strategy for development of CNS edema therapies.

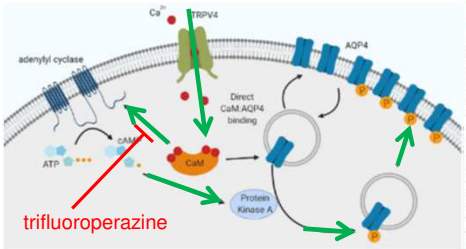

Figure 5. AQP4 Subcellular Relocalization Drives Cytotoxic Edema: The Proposed Roles of CaM and PKA

For a Figure360 author presentation of this figure, see https://doi.org/10.1016/j.cell.2020.03.037.

Following hypoxic insult, failure in Na^+, K^+, and Cl^- pumps in the plasma membrane leads to osmotic dysregulation. The mechanosensitive TRPV4 channel facilitates an influx of Ca^{2+} ions into astrocytes, which activates CaM. CaM interacts with an adenylyl cyclase, activating cyclic AMP (cAMP)-dependent PKA, which phosphorylates AQP4 at Ser276, causing it to relocalize to the plasma membrane. CaM interacts directly with AQP4; this regulatory interaction drives AQP4 subcellular relocalization (created with https://biorender.com).

Cell

Article

Targeting Aquaporin-4 Subcellular Localization to Treat Central Nervous System Edema

Graphical Abstract

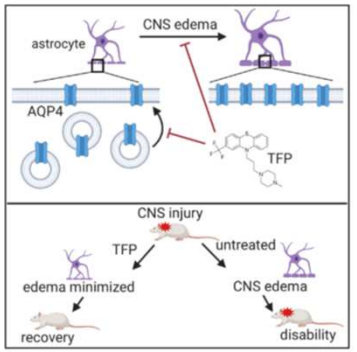

Authors

Philip Kitchen, Mootaz M. Salman, Andrea M. Halsey, ..., Zubair Ahmed, Alex C. Conner, Roslyn M. Bill

Correspondence

z.ahmed.1@bham.ac.uk (Z.A.), a.c.conner@bham.ac.uk (A.C.C.), r.m.bill@aston.ac.uk (R.M.B.)

In Brief

Modulating the subcellular localization of the water channel protein AQP4 may be a therapeutic option for treatment of brain and spinal cord edemas.

Kitchen et al., 2020, Cell 181, 784–799
May 14, 2020 © 2020 The Author(s). Published by Elsevier Inc.
https://doi.org/10.1016/j.cell.2020.03.037

CellPress

Clinically Approved Heterocyclics Act on a Mitochondrial Target and Reduce Stroke-induced Pathology

Irina G. Stavrovskaya,[1] Malini V. Narayanan,[2] Wenhua Zhang,[2] Boris F. Krasnikov,[1] Jill Heemskerk,[3] S. Stanley Young,[4] John P. Blass,[1,5] Abraham M. Brown,[1,6] M. Flint Beal,[5] Robert M. Friedlander,[2] and Bruce S. Kristal[1,5,6]

[1]*Dementia Research Service, Burke Medical Research Institute, White Plains, NY 10605*
[2]*Neuroapoptosis Laboratory, Department of Neurosurgery, Brigham and Women's Hospital and Harvard Medical School, Boston, MA 02115*
[3]*Technology Development, National Institute of Neurological Disorders and Stroke, Bethesda, MD 20892*
[4]*CGStat LLC, Raleigh, NC 27607*
[5]*Department of Neurology and Neuroscience and* [6]*Department of Biochemistry, Weill Medical College of Cornell University, New York, NY 10021*

J. Exp. Med. © The Rockefeller University Press
Volume 200, Number 2, July 19, 2004 211–222
http://www.jem.org/cgi/doi/10.1084/jem.20032

Drug name	Drug class	PT	p-value	CAL	PLA_2	Cerebral IR	Cell
Trifluoperazine	Antipsychotic	4.28 ± 1.56	<0.0001	20	ND	74, 75	76, 78
Methiothepin	Other	3.61 ± 0.79	<0.0001	78	54		
Promethazine	Antihistaminic	3.56 ± 0.97	<0.0001	84	97	[a]	[b]
Triflupromazine	Antipsychotic	3.41 ± 1.21	<0.0001	70	75		
Clomipramine	Antidepressant	3.33 ± 1.03	<0.001	80	39	77, 79	
Flufenazine	Antihistaminic	3.32 ± 1.54	<0.01	73	72		
Chlorprothixene	Antipsychotic	3.30 ± 1.24	<0.01	111	94		
Nortriptyline	Antidepressant	3.16 ± 1.12	<0.01	77	81	[c]	78, 80
Promazine	Antipsychotic	3.14 ± 0.83	<0.01	74	38		
Thioridazine	Antipsychotic	3.14 ± 1.03	<0.0001	84	76		
Mefloquine	Other	3.09 ± 0.50	<0.0001	37	45		
Desipramine	Antidepressant	3.08 ± 0.95	<0.0001	52	54	79, 81	80, 82
Chlorpromazine	Antipsychotic	2.98 ± 0.74	<0.001	82	69	75, 81, 82	83, 84
Prochlorperazine	Antipsychotic	2.96 ± 1.05	<0.0001	66	40		
Propiomazine	Other	2.88 ± 0.89	<0.01	111	47		
Pimethixene	Antihistaminic	2.79 ± 0.99	0.001	26	33		
Perphenazine	Antipsychotic	2.74 ± 0.42	<0.01	103	58		
Amitriptyline	Antidepressant	2.64 ± 0.77	<0.0001	72	80		78, 80
Amoxepine	Antidepressant	2.50 ± 0.60	<0.001	45	29		
Maprotiline	Antidepressant	2.42 ± 0.56	<0.001	50	10		
Quinacrine	Other	2.42 ± 1.21	<0.05	121	43	85–87	88, 89
Penicianine	Antipsychotic	2.36 ± 1.17	<0.05	84	47		
Ethopropazine	Other	2.30 ± 0.69	<0.01	62	31		
Mianserin	Other	2.21 ± 0.67	<0.001	37	23	90, 92	
Cyclobenzaprine	Other	2.12 ± 0.38	<0.0001	87	80		
Imipramine	Antidepressant	2.10 ± 0.50	<0.01	ND	79		78, 80
Clozapine	Antipsychotic	2.07 ± 0.63	<0.01	96	106	91, 93	
Doxepin	Antidepressant	1.68 ± 0.56	<0.05	68	87	79, 81	
Loratadine	Antihistaminic	1.04 ± 0.35	NS	251	93		
Thiothixene	Antipsychotic	1.03 ± 0.21	NS	71	115		
Propantheline	Other	0.84 ± 0.39	NA	87	76	None identified	
Pirenzepine	Other	0.70 ± 0.30	NA	485	45